Twofold enhancement of the hidden-order/large-moment antiferromagnetic phase boundary in the $URu_{2-x}Fe_xSi_2$ system

N. Kanchanavatee, M. Janoschek,* R. E. Baumbach,* J. J. Hamlin, D. A. Zocco, K. Huang, and M. B. Maple†
Department of Physics, University of California, San Diego, La Jolla, California 92093, USA
(Received 2 August 2011; revised manuscript received 30 November 2011; published 16 December 2011)

Electrical resistivity, specific heat, and magnetization measurements on $URu_{2-x}Fe_xSi_2$ reveal a twofold enhancement of the "hidden-order" (HO)/large-moment antiferromagnetic (LMAFM) phase boundary $T_0(x)$. The $T_0(P_{ch})$ curve, obtained by converting x to "chemical pressure" P_{ch}, is strikingly similar to the $T_0(P)$ curve, where P is applied pressure, for URu_2Si_2 both exhibit a "kink" at 1.5 GPa and a maximum at ~7 GPa. This similarity suggests that the HO-LMAFM transition at 1.5 GPa in URu_2Si_2 occurs at $x \approx 0.2$ ($P_{ch} \approx 1.5$ GPa) in $URu_{2-x}Fe_xSi_2$. $URu_{2-x}Fe_xSi_2$ provides an opportunity for studying the HO and LMAFM phases with methods that probe the electronic structure [e.g., scanning tunneling microscopy (STM), angle-resolved photoemission spectroscopy (ARPES), and point-contact spectroscopy (PCS)] but cannot be used under pressure.

DOI: 10.1103/PhysRevB.84.245122 PACS number(s): 71.10.Hf, 71.27.+a, 74.70.Tx

I. INTRODUCTION

The strong electronic correlations that arise from the hybridization of localized d- or f-electron and conduction electron states in compounds containing transition metal, lanthanide, or actinide ions with partially filled d- or f-electron shells often lead to the emergence of novel electronic ground states such as heavy fermion metals, complex magnetic order, quadrupolar order, non-Fermi-liquid (NFL) behavior, and unconventional superconductivity (SC).[1] A prime example of such emergent behavior is the "hidden-order" (HO) phase in the heavy fermion compound URu_2Si_2 that occurs below $T_0 = 17.5$ K and coexists with SC below $T_c = 1.5$ K.[2–4] The specific-heat anomaly that accompanies the HO phase transition is reminiscent of a second order BCS-like mean field transition that opens a gap $\Delta \approx 130$ K over about 40% of the Fermi surface (FS) due to a charge or spin density wave.[3] However, the small antiferromagnetic magnetic moment of only ~0.03 μ_B/U derived from neutron scattering experiments[5,6] cannot account for the entropy of ~0.2Rln(2) associated with the specific-heat anomaly.[5] The terminology HO[7] refers to the ordered phase responsible for the striking specific heat anomaly whose order parameter (OP) has eluded identification for nearly three decades.

The search for the OP of the HO phase has attracted an enormous amount of attention. A multitude of models for the HO have been proposed, which can be roughly divided into two groups, one based on a local OP and another involving order that occurs in momentum space (see Ref. 8 and references therein). ARPES,[9] STM,[10,11] and PCS[12] studies show that upon cooling into the HO phase, the electronic structure is reorganized and a heavy quasiparticle band shifts below the Fermi level, where the crossing with a light hole-like band at $Q^* = \pm 0.3\pi/a$ leads to the formation of a hybridization gap $\Delta_{Q^*} = 5$ meV. It was suggested that the HO may be a hybridization wave where Δ_{Q^*} is the corresponding OP.[8,13] The recent proposal of a modulated spin liquid lies between the extremes of local and itinerant OPs.[14]

The hybridization between localized f and conduction electron states may be tuned by varying a control parameter such as composition x, pressure P, or magnetic field H, allowing information about the electronic ground state to be extracted from various measurements. This approach has been applied extensively to URu_2Si_2, revealing rich T vs x, P, and H phase diagrams with a plethora of competing electronic ground states. Through the application of pressure, it has been shown that the magnetic structure in the HO phase is identical to that of a larger moment antiferromagnetic (LMAFM) phase that emerges at critical pressures $P_c \geqslant 0.5$–1.5 GPa[15] (see also Ref. 16 and references therein). There is strong evidence that the HO-LMAFM phase transition is of first order,[17] leading to the widely held view that the magnetic structure in the HO phase is due to a small amount of the LMAFM phase induced by strain.[6] However, other researchers believe that the small magnetic moment in the HO phase is intrinsic since its onset temperature coincides with that of the HO, and it is present in samples with residual resistivities that vary by as much as two orders of magnitude.[18] In fact, some models predict that antiferromagnetic order in the HO phase is intrinsic.[19] Tuning with H revealed several high field quantum phases that exhibit NFL behavior.[20] Finally, substitution of other transition metals for Ru generally leads to suppression of the HO,[21] and, for example, yields a LMAFM phase for Rh substitution[22] and an itinerant ferromagnetic phase for Mn, Tc, or Re substitutions,[23,24] accompanied by NFL behavior deep in the ferromagnetic state for Re.[25,26]

In this paper we demonstrate that substitution of the smaller Fe ions for Ru ions in URu_2Si_2 provides a new approach for studying the properties of the HO phase. Measurements of electrical resistivity ρ, specific heat C, and magnetization M on a series of polycrystalline samples of $URu_{2-x}Fe_xSi_2$ with Fe concentrations x ranging from $x = 0$ to 2 reveal a remarkable phase diagram. The most salient characteristics of this phase diagram are (1) the striking shape of the T–x phase boundary $T_0(x)$ separating the paramagnetic phase from the ordered phases (HO and/or LMAFM) with a more than twofold enhancement of T_0. (2) Features in $T_0(x)$, similar to those in the T–P phase diagram of pure URu_2Si_2, that appear to be generated by "chemical pressure" (reduction in the unit cell volume) arising from the substitution of the smaller isoelectronic Fe ions for Ru ions, particularly the kink at $x = 0.2$ that maybe related to a HO-LMAFM transition. (3) Increase

of the energy gap Δ of the HO phase and the amount of the FS gapped by the HO phase with increasing x, inferred from fits of a theoretical model with gapped excitations to the low temperature electrical resistivity and specific heat. (4) Coexistence of SC and HO for $x \lesssim 0.075$. (5) The possible existence of a quantum critical point at $x \approx 1.3$ where the HO and/or LMAFM are suppressed to 0 K. This phase diagram may provide new opportunities for establishing the identity of the OP of the HO phase.

II. EXPERIMENTAL METHODS

Polycrystalline samples of $URu_{2-x}Fe_xSi_2$ $(0 \leqslant x \leqslant 2)$ were prepared by arc melting high-purity starting materials (U, 99.9%; Ru, 99.95%; Fe, 99.99%; Si, 99.9999%) on a water-cooled copper hearth in a zirconium gettered argon atmosphere. After arc melting, each sample was flipped over and remelted. This process was repeated five times in order to ensure homogeneous mixing of the starting materials. This was followed by annealing in vacuum at 900 °C for 5 days. The crystal structure was verified by means of x-ray powder diffraction (XRD) using a Bruker D8 Discover x-ray diffractometer with Cu-$K\alpha$ radiation. The resulting XRD patterns were fitted via Rietveld refinement[27] using the GSAS + EXPGUI software package.[28,29] The chemical composition was investigated by means of energy dispersive x rays (EDX) using a FEI Quanta 600 scanning electron microscope equipped with an INCA EDX detector from Oxford instruments. Electrical resistivity measurements were performed using a home-built probe in a liquid ^{4}He Dewar for temperatures $1 \leqslant T \leqslant 300$ K by means of a standard four-wire technique at ~16 Hz using a Linear Research LR700 ac resistance bridge. For selected samples, $\rho(T)$ was also measured down to $T = 0.05$ K in an Oxford Kelvinox-300 ^{3}He-^{4}He dilution refrigerator. Magnetization measurements were made for $2 \leqslant T \leqslant 300$ K and in magnetic fields $H = 0.1$ T using a Quantum Design SQUID magnetometer. Specific heat measurements were performed for $1.8 \leqslant T \leqslant 50$ K in a Quantum Design physical property measurement system semiadiabatic calorimeter using a heat-pulse technique.

III. RESULTS

A. Crystal structure and sample quality

UFe_2Si_2 is isostructural with URu_2Si_2 (space group $I4/mmm$) and, correspondingly, we find that samples for the entire range of Fe substitutions $0 \leqslant x \leqslant 2$ can be described in the same space group and there are no indications of miscibility gaps. The typical goodness of fit extracted from the Rietveld refinement indicated by χ^2 ranged from 4 to 10; Fig. 1(a) illustrates the quality of the refinement that was typically achieved. As shown in Fig. 1(b), the lattice parameters a and c decrease with increasing Fe concentration, although the decrease of c is much smaller. Overall, the unit cell volume of $URu_{2-x}Fe_xSi_2$ decreases linearly with x [Fig. 1(c)], as expected from the smaller size of Fe relative to Ru ions. Furthermore, the combined EDX/XRD refinement indicated correct composition within the accuracy of the measurement [see Fig. 1(d)] and no evidence of impurities, except for samples with $x = 0.70$, 0.80, and 1.00, where we identified a small amount of UO impurity phase of only a few percent.

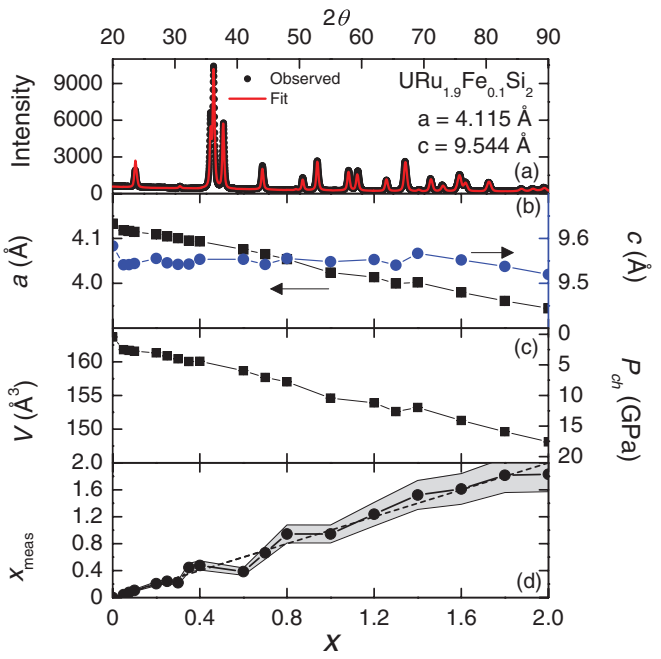

FIG. 1. (Color online) Results of the Rietveld refinement and EDX analysis. (a) X-ray diffraction pattern for $URu_{2-x}Fe_xSi_2$ with Fe concentration $x = 0.1$. Black dots represent the data, and the red solid line is the fit to the data. (b) Lattice parameters a and c vs nominal Fe concentration x. (c) Unit cell volume V vs x. For the axis on the right side the unit cell volume was converted to chemical pressure (see text, Sec. IV). (d) Fe concentration x_{meas}, determined from EDX measurements, vs x. The shaded region is the error in x_{meas} due to the accuracy of the EDX measurement.

B. Electrical resistivity

The measurements of the electrical resistivity ρ further emphasize that polycrystalline samples of high quality have been obtained. The residual resistivity ratio (RRR), defined as $\rho(300\text{ K})/\rho(2\text{ K})$, for the pure URu_2Si_2 and UFe_2Si_2 samples are 100 and 220, respectively. For increasing Fe concentration x, however, the RRR drops rapidly to approximately 5, presumably due to the disorder introduced by the Fe substitution.

The superconducting critical temperature T_c is rapidly suppressed by Fe substitution and SC is not observed for $x \gtrsim 0.075$ down to 50 mK. As illustrated in Fig. 2, the transition at $T_0(x)$ into the HO in $URu_{2-x}Fe_xSi_2$ is visible as a small peak in $\rho(T)$ or, alternatively, an inflection point in $d\rho/dT$. $T_0(x)$ increases with x from 17.5 K at $x = 0$ to a maximum value of 42 K at $x \approx 0.8$. We note that, as will be discussed in more detail in Sec. IV of the paper, our data indicates a phase transition from the HO into the LMAFM phase at $x \approx 0.2$. For $x > 0.8$, $T_0(x)$ decreases with x and disappears at $x \approx 1.3$. Additionally, starting from $x = 0.075$, the peak in $\rho(T)$ that we associate with T_0 begins to broaden significantly. This broadening is more clearly visible in $d\rho/dT$ as shown in Fig. 2(e). We have identified the onset of the transition to the HO phase T_0' as the upper inflection point in $d\rho/dT$ as marked with the empty arrows. Starting from

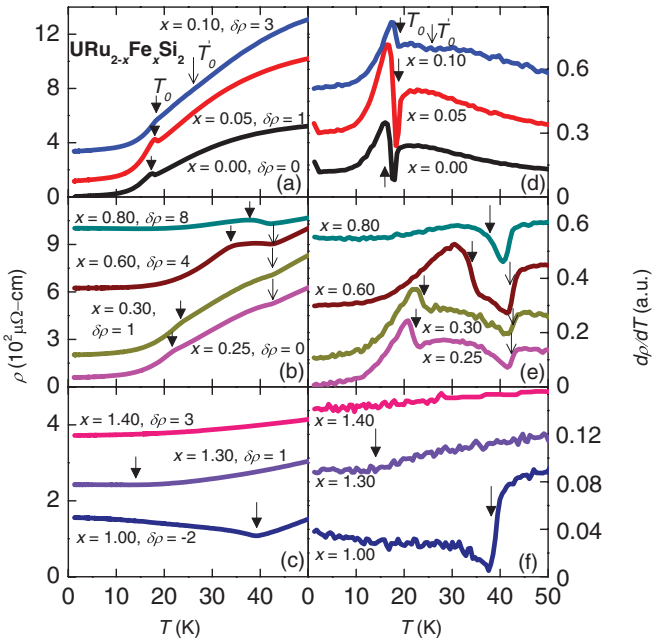

FIG. 2. (Color online) (a)–(c) Electrical resistivity ρ vs temperature T for $URu_{2-x}Fe_xSi_2$. For clarity of presentation, only selected values of x are shown. Each data set is shifted by $\delta\rho$, the values of which are indicated in the figure. (d)–(f) Derivative of ρ with respect to T, $d\rho/dT$, vs T. T_0 marks the transition to the HO/LMAFM phases and T_0' is the onset of the transition (see text).

$x = 0.8$, $\rho(T)$ also develops a low T minimum that "tracks" T_0, where the corresponding low T upturn of ρ is most pronounced for $x = 1$ and disappears when T_0 is suppressed to zero for $x \to 1.3$ [Figs. 2(c) and 2(f)].

C. Magnetization

The HO transition in $M(T)$ is manifested as a change of slope [Fig. 3(a)] that closely tracks $T_0(x)$, as observed in $\rho(T)$. Alternatively, the HO transition can be identified as a peak in dM/dT [Fig. 3(b)]. The signature of the onset of the HO at T_0' in $M(T)$ is weak and only discernible for $x = 0.60$ as a small kink that appears as an inflection point in dM/dT. A low T upturn is observed in $M(T)$ for $x \leqslant 1.0$ and $T < 5$ K, which becomes more pronounced for $x \geqslant 1.0$ as it moves to higher T.

D. Specific heat

In Fig. 4 we show the electronic specific heat $C_e(T)$ that was determined for all x by subtracting the phonon contribution $C_{\rm ph}(T)$ of UFe_2Si_2. This method should yield a good estimate of the phonon contribution for all values of x since the end member compounds are isostructural and UFe_2Si_2 is reported to be a Pauli paramagnet down to 0.2 K.[30] Using only a Debye function, we were not able to account correctly for the phonon contribution over the entire T range measured.

For URu_2Si_2, the HO transition appears in $C_e(T)/T$ as a jump at T_0 whose shape is reminiscent of a second-order BCS-type mean-field transition. With increasing x, this anomaly moves to higher temperatures, while the size of the jump $\Delta C_e/T$ decreases and disappears at $x \approx 0.8$. In

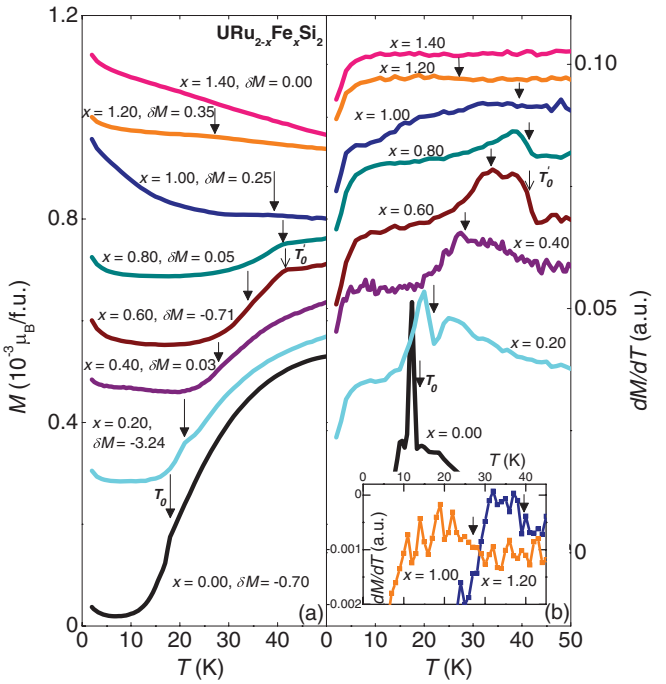

FIG. 3. (Color online) (a) Magnetization M vs temperature T for $URu_{2-x}Fe_xSi_2$ in a magnetic field $H = 0.1$ T. For clarity of presentation, only selected values of x are shown. Each data set is shifted by δM, the values of which are indicated in the figure. (b) Derivative of M with respect to T, dM/dT, vs T. T_0 and T_0' are the ordering temperature and the onset to the hidden order (see text), respectively. Inset: Detail of dM/dT for $x = 1.0$ and 1.2.

agreement with $\rho(T)$ and $M(T)$ results, the transition broadens significantly, leading to a shoulder in the $C(T)$ peak for $x \geqslant 0.075$. Here we define the shoulder at T_0' as the onset of the transition to the HO and LMAFM phases, respectively.

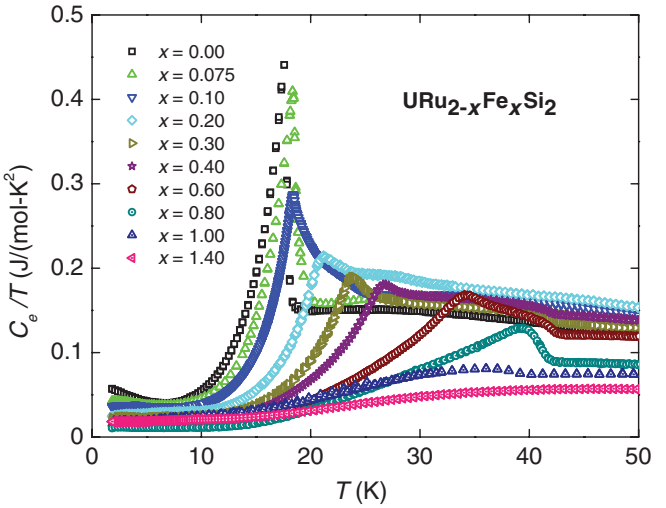

FIG. 4. (Color online) Electronic specific heat C_e divided by temperature T vs T for $URu_{2-x}Fe_xSi_2$. For clarity of presentation, only selected values of x are shown.

IV. DISCUSSION

A. Phase diagram and HO-LMAFM phase transition

In Fig. 5(a) we have summarized the results of the $\rho(T)$, $M(T)$, and $C(T)$ measurements discussed in the previous section in a phase diagram showing the HO transition temperature T_0 vs Fe concentration x. $T_0(x)$ increases linearly with x from 17.5 K at $x = 0$ to 21 K at $x \approx 0.2$, exhibits a kink at $x \approx 0.2$, and then increases linearly with a larger slope to a maximum value of 42 K at $x \approx 0.8$; thereafter, $T_0(x)$ decreases with x and vanishes at $x \approx 1.3$. This behavior is quite reminiscent of the T vs P phase diagram observed for URu_2Si_2. Due to the differences in the atomic radii, substitution of isoelectronic ions often induces a change in the unit cell volume that may be interpreted as a "chemical pressure" P_{ch}. The linear decrease of the unit cell volume of $URu_{2-x}Fe_xSi_2$ with increasing Fe concentration x [see Fig. 1(c)] established by our XRD analysis is consistent with that view. We have therefore used the variation of the unit cell volume with x to estimate the value of P_{ch} corresponding to each concentration x according to the isothermal compressibility $\kappa_T = 5.2 \times 10^{-3}$ GPa^{-1} of

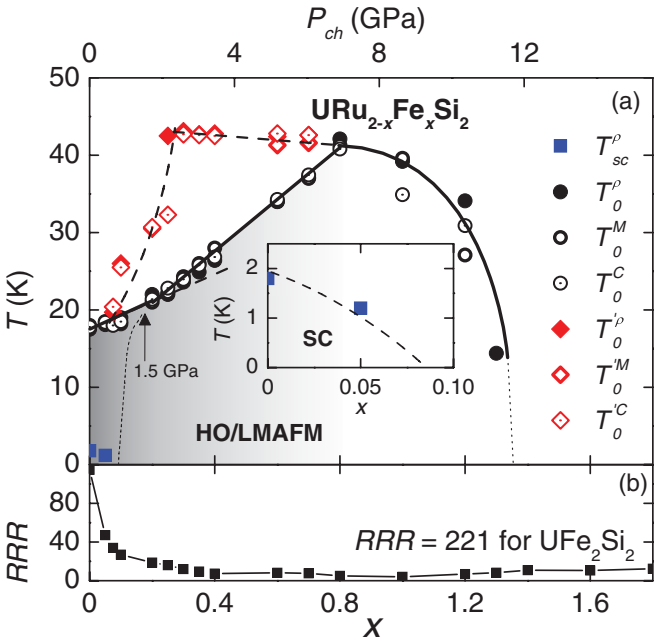

FIG. 5. (Color online) (a) Temperature T vs Fe concentration x phase diagram of $URu_{2-x}Fe_xSi_2$, constructed from electrical resistivity (ρ, filled symbols), specific heat (C, empty-dotted symbols), and magnetization (M, empty symbols) measurements. The T–x phase boundary $T_0(x)$ (solid black line) separates the ordered phases (HO and LMAFM) from the paramagnetic phase. The superconducting critical temperature T_c and the transition temperature T_0 and onset temperature T_0' (see text) of the ordered phases are denoted by blue squares, black circles, and red diamonds, respectively. The dashed bold line is an extrapolation of $T_0(x)$ to emphasize the kink at $x \approx 0.2$. The Fe concentration x was converted to "chemical pressure" P_{ch} on the top horizontal axis (see text). The thin dashed line is the HO-LMAFM transition in URu_2Si_2 as observed under pressure.[16] The inset highlights the region around the superconducting phase. (b) Residual resistivity ratio RRR, defined as $\rho(300\text{ K})/\rho(2\text{ K})$, vs x.

URu_2Si_2 reported in Ref. 31 [see right axis of Fig. 1(c) and top horizontal axis in Fig. 5(a)]. We note, however, that the conversion depends on the value chosen for κ_T, and that literature values vary from 2×10^{-3} (Ref. 15) to 7.3×10^{-3} GPa^{-1} (see references in Ref. 31). It is interesting that the kink in the T–P_{ch} phase boundary $T_0(P_{ch})$ at 1.5 GPa and the slopes of $T_0(P_{ch})$ of 2.1 and 3.9 K/GPa below and above the kink are consistent with the values of the T–P phase boundary $T_0(P)$ of pure URu_2Si_2 (1.3 and 3.8 K/GPa, respectively), where the kink occurs at the transition between the HO and LMAFM phases. This similarity suggests that the kink in $T_0(P_{ch})$ [and, in turn, $T_0(x)$] is associated with a transition from the HO to the LMAFM phase as indicated by the thin dashed line in Fig. 5(a) that marks the HO-LMAFM transition in URu_2Si_2, according to recent neutron scattering studies under pressure.[16] In addition, the chemical pressure $P_{ch} \approx 0.8$ GPa at which SC is suppressed to zero agrees well with previous high pressure studies,[16] while the maximum value of $T_0 \approx 42$ K and the value of $P_{ch} \approx 7$–8 GPa at which it occurs, are consistent with the high pressure study of URu_2Si_2 by Iki *et al.*[32]

The low T upturns that are observed in $\rho(T)$ and $M(T)$ for $x \to 1.3$ where T_0 is suppressed to zero [Figs. 2(c), 2(f), and 3] are reminiscent of the quantum critical scenario recently reported for chromium where spin density wave order breaks down at the critical pressure $P_c = 9.71$ GPa.[33] This suggests that a quantum critical point (QCP) may be located at $x \approx 1.3$ in $URu_{2-x}Fe_xSi_2$ due to suppression of the LMAFM phase.

The established T vs P_{ch} phase diagram also offers an explanation for the broadening of the HO transition that is mainly manifested in the $\rho(T)$ and $C_e(T)$ data. We believe that the broadening of the transition is due to small Fe concentration inhomogeneities that may generate appreciable internal strain. From high pressure studies on URu_2Si_2, it is known that the HO transition is very sensitive to strain.[6,16] This scenario is corroborated by the residual resistivity ratio RRR that drops rapidly with increasing x from 100 at $x = 0$, and then levels off at $x = 0.075$ where the broadening of the HO transition first appears, indicating additional scattering due to disorder [Fig. 5(b)]. It is noteworthy that the value of T_0' saturates rapidly at ~42 K corresponding to the maximum of $T_0(x)$. Accordingly, the width of the transition again decreases when T_0 reaches its maximum at $x = 0.8$. The weak signature of the onset of the HO/LMAFM phases, T_0', in the $M(T)$ measurements indicates that the inhomogeneous regions occupy only a small volume fraction, as further corroborated by XRD and EDX measurements, which show that the samples are formed with the correct composition. We therefore attribute the broadening of the transition to the extreme sensitivity of URu_2Si_2 to strain.[6,16] Preliminary results on single crystals of $URu_{2-x}Fe_xSi_2$ show no broadening of the transition, supporting this interpretation.

B. Stabilization of the HO phase

In order to investigate the stabilization of the HO phase by the substitution of Fe with Ru, manifested in the increase of T_0 with x, in more detail, we have performed fits of relevant theoretical models to the features in $\rho(T)$ and $C_e(T)$ that characterize the HO phase. As demonstrated for URu_2Si_2

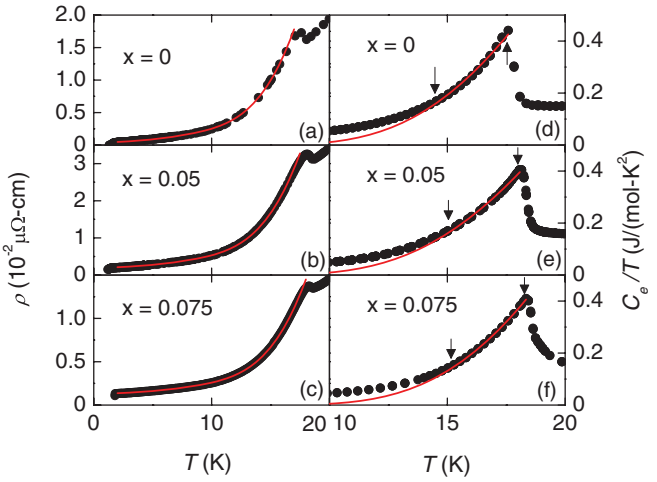

FIG. 6. (Color online) Fits of the low temperature electrical resistivity $\rho(T)$ and electronic specific heat $C_e(T)$ to a theoretical model with gapped magnetic excitations (see text) for several Fe concentrations x. In the HO phase, the $\rho(T)$ data [(a)–(c)] have been fitted using Eq. (2) whereas the $C_e(T)$ data [(d)–(f)] have been fitted using Eq. (3). Black circles represent the data, red solid lines the resulting fits, and arrows the fitting ranges.

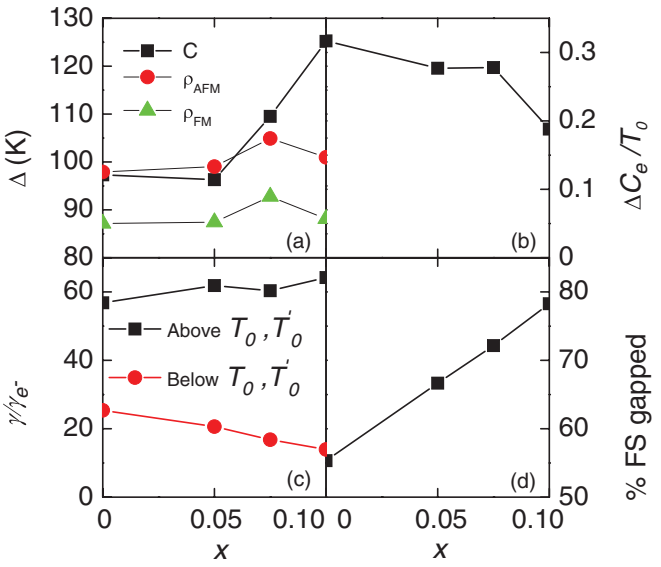

FIG. 7. (Color online) (a) Energy gap Δ that opens on the FS due to the onset of the HO phase as determined via fits to the low temperature electrical resistivity $\rho(T)$ (red circles and green triangles corresponding to a theoretical model with gapped antiferromagnetic and ferromagnetic excitations, respectively; see text) and electronic specific heat $C_e(T)$ (black squares) vs x (see text and Fig. 6). (b) Jump in C_e at the transition to the HO phase divided by T_0, $\Delta C_e/T_0$, vs Fe concentration x. (c) Ratio of measured and calculated free electronic specific-heat coefficients γ and γ_{e^-} vs x for T above and below T_0 (and T_0'), respectively. (d) Fraction of the FS that is gapped below the HO transition vs x.

at ambient pressure,[34] under pressure,[35] and substituted with other elements,[36] $\rho(T)$ in the HO phase is well described by the expression

$$\rho(T) = \rho_0 + AT^2 + B\Delta T\left(1 + 2\frac{T}{\Delta}\right)e^{-\frac{\Delta}{T}}, \qquad (1)$$

which includes the residual resistivity ρ_0, a Fermi liquid term AT^2, and an electron-magnon scattering contribution due to spin excitations with an energy gap Δ. We note, however, that some ambiguity about the expression used to describe the electrical resistivity in the HO phase exists in the literature. Equation (1) was originally derived to describe electron-magnon scattering due to ferromagnetic magnons.[37] However, the magnons observed in URu_2Si_2 are of antiferromagnetic nature and the following expression should, in principle, be used to fit the electrical resistivity:[38]

$$\rho(T) = \rho_0 + AT^2 + B\Delta^2\sqrt{\frac{T}{\Delta}} \times\left[1 + \frac{2}{3}\left(\frac{T}{\Delta}\right) + \frac{2}{15}\left(\frac{T}{\Delta}\right)^2\right]e^{-\frac{\Delta}{T}}. \qquad (2)$$

The resulting fits of $\rho(T)$ using Eq. (2) are shown in Figs. 6(a)–6(c). The differences in the values extracted for Δ via fits to the low temperature $\rho(T)$ data of Eqs. (1) and (2), respectively, are small because the exponential term that contains the gap Δ is the dominant term in both expressions, and thus qualitatively identical behavior is observed. In order to facilitate the comparison to previously published data, we provide the values of Δ derived from both expressions in Fig. 7(a). We emphasize that the values for Δ extracted by means of Eq. (2) also match much better with the values for the gap obtained from fits of the low temperature specific heat [see below and Fig. 7(a)]. Since for $x > 0.1$, the low temperature electrical resistivity flattens considerably, it becomes unreasonable to describe the $\rho(T)$ data with both the Fermi liquid and exponential contributions; therefore, we have limited the fits to the $\rho(T)$ data for $x \leqslant 0.1$. The extracted size of the HO gap increases moderately with increasing x up to $x = 0.075$, after which it saturates again [Fig. 7(a)], suggesting that the HO phase is at least initially stabilized by introducing Fe into URu_2Si_2.

Below the HO transition, the $C_e(T)$ data can be described by the expression

$$C_e(T) = A\exp(-\Delta/T), \qquad (3)$$

where Δ is the gap that opens over the FS (Ref. 3). The fits of Eq. (3) to the $C_e(T)$ data are displayed in Figs. 6(d)–6(f) in the form of $C_e(T)/T$ vs T plots. Since the shape of the HO anomaly in C/T deviates increasingly from a BCS form with increasing x, we have limited this analysis to $x \leqslant 0.1$, as well. As indicated in Fig. 7(a), the size of Δ increases with increasing x. At the same time, the jump in C_e at the transition to the HO phase divided by T_0 remains approximately constant with increasing x and only decreases significantly for $x \geqslant 0.1$. In order to approximate the fraction of the FS that is gapped, we have estimated the electronic specific-heat coefficient γ_n by linearly extrapolating C_e/T from above T_0 and T_0' to $T = 0$, and, accordingly, γ_0 for the gapped FS by linearly extrapolating the C_e/T data from below the transition to $T = 0$, following the method described in Ref. 3. In Fig. 7(c), both γ_n and γ_0 are compared to γ_{e^-} for the ungapped state, calculated for conduction electrons with the free electron mass. At $x = 0$ we find that 55% of the FS is gapped, in agreement with previous reports.[3] With increasing x, γ_n increases, whereas γ_0 decreases, leading

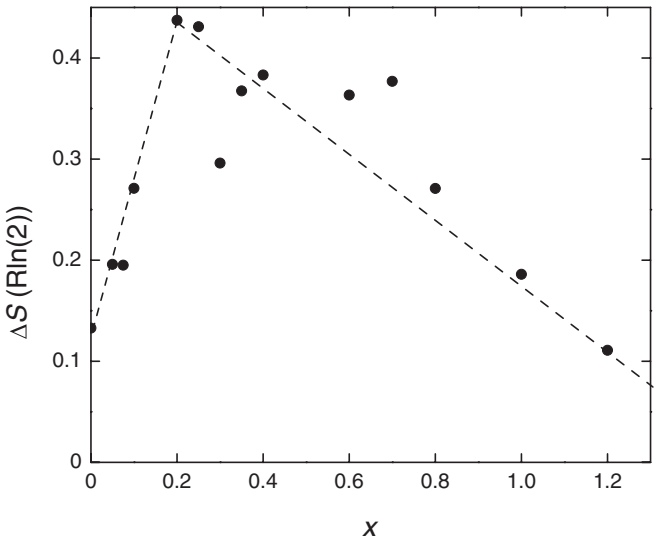

FIG. 8. The difference in entropy between the normal state and the hidden-order state ΔS vs Fe concentration x.

to an increase of the fraction of the FS that is gapped, which at $x = 0.1$ reaches a value of 0.8 [Fig. 7(d)]. It is noteworthy that the change of shape of the HO anomaly occurs at $x = 0.2$, where $T_0(x)$ exhibits a kink. In addition, extrapolating the fraction of the FS that is gapped to higher values of x suggests that the FS will be entirely gapped at $x \approx 0.2$.

To further elucidate this point, we have calculated the entropy for $URu_{2-x}Fe_xSi_2$ as a function of x. Shown in Fig. 8 is the difference of entropy between the normal state and the hidden-order state ΔS vs x. Here the entropy of the normal state was estimated by linearly extrapolating C_e/T from above the HO transition to zero and computing the area below that line, whereas the entropy in the HO state was calculated by integrating C_e/T up to T_0. ΔS peaks at $x = 0.2$, demonstrating that the largest amount of entropy is removed from the system due to onset of the HO phase for $x = 0.2$, again indicating that the HO state is stabilized with increasing Fe concentration for $0 \leqslant x \leqslant 0.2$. The decrease in ΔS for $x > 0.2$ provides further support for the possibility of a transition from the HO to LMAFM state at $x = 0.2$.

V. CONCLUDING REMARKS

In summary, we have established the phase diagram for $URu_{2-x}Fe_xSi_2$ over the entire range of Fe compositions from $x = 0$ to 2 (Fig. 5). Particularly noteworthy is a more than twofold increase of T_0 from 17.5 K at $x = 0$ to 42 K at $x = 0.8$. Here the striking similarities of the effect of chemical pressure and external pressure on URu_2Si_2 suggest that for $x \geqslant 0.2$ (corresponding to $P_{ch} = 1.5$ GPa), $T_0(x)$ marks the phase boundary to an ordered phase that is different from the HO phase and is presumably similar to the LMAFM phase identified in URu_2Si_2 for pressures $P \geqslant 1.5$ GPa. However, in the experiments reported herein, it was not possible to determine the phase boundary between the HO and LMAFM phases in the ordered region of the phase diagram. This will require neutron diffraction measurements that are able to determine the magnetic structure and ordered magnetic moment as a function of Fe concentration x. Both the electrical resistivity and the specific heat results demonstrate that, at least up to $x = 0.1$, the HO is further stabilized as indicated by the increasing size of both the HO gap and the fraction of gapped FS. Furthermore, circumstantial evidence suggests that the HO is stabilized against thermal fluctuations even up to $x \approx 0.2$: (1) the shape of the T_0 anomaly in the specific heat changes at $x = 0.2$, (2) the extrapolated gapped fraction of the FS approaches 1 as $x \to 0.2$, (3) the difference of entropy between the normal state and the HO state ΔS peaks at $x = 0.2$, and (4) the similarity of $T_0(P_{ch})$ and $T_0(P)$, in conjunction with the kink in $T_0(x)$ at $x = 0.2$, indicates that the HO phase extends to $x = 0.2$. We note that the application of chemical pressure to URu_2Si_2 extends the range of experiments that may be used to study the HO to methods, such as STM, ARPES and PCS, that are generally not available in combination with applied pressure, but hold the promise of new insights into the HO. In particular, this will be important for testing models for the HO based on an itinerant OP such as the recently proposed hybridization wave.[8,13] We note, however, that high quality single crystals are required for these experiments. Using single crystal samples will also mitigate the problem of disorder that is observed for increasing Fe concentrations, thereby reducing the broadening of the HO transition. This has been verified with preliminary experiments on single crystals of $URu_{2-x}Fe_xSi_2$ that will be published elsewhere. Finally, the apparent QCP that is indicated by low temperature divergences in the electrical resistivity and magnetization at $x = 1.3$, where T_0 extrapolates to zero, may also shed some light onto the delicate interplay between HO and the LMAFM phase.

ACKNOWLEDGMENTS

Sample synthesis and characterization were funded by the US DOE under Grant No. DE FG02-04ER46105. Low-temperature measurements were supported by the NSF under Grant No. 0802478. N.K. and M.J. acknowledge financial support through the Royal Thai Government Scholarship and by the Alexander von Humboldt Foundation, respectively.

*Present Address: Condensed Matter and Magnet Science group, Los Alamos National Laboratory, Los Alamos, New Mexico 87545.
†Corresponding author: mbmaple@ucsd.edu

[1]M. B. Maple, R. E. Baumbach, N. P. Butch, J. J. Hamlin, and M. Janoschek, Low Temp. Phys. **161**, 4 (2010).
[2]T. T. M. Palstra, A. A. Menovsky, J. van den Berg, A. J. Dirkmaat, P. H. Kes, G. J. Nieuwenhuys, and J. A. Mydosh, Phys. Rev. Lett. **55**, 2727 (1985).
[3]M. B. Maple, J. W. Chen, Y. Dalichaouch, T. Kohara, C. Rossel, M. S. Torikachvili, M. W. McElfresh, and J. D. Thompson, Phys. Rev. Lett. **56**, 185 (1986).
[4]W. Schlabitz, J. Baumann, B. Pollit, U. Rauchschwalbe, H. M. Mayer, U. Ahlheim, and C. D. Bredl, Z. Phys. B **62**, 171 (1986).
[5]C. Broholm, J. K. Kjems, W. J. L. Buyers, P. Matthews, T. T. M. Palstra, A. A. Menovsky, and J. A. Mydosh, Phys. Rev. Lett. **58**, 1467 (1987).

[6]P. G. Niklowitz, C. Pfleiderer, T. Keller, M. Vojta, Y.-K. Huang, and J. A. Mydosh, Phys. Rev. Lett. **104**, 106406 (2010).
[7]B. Luethi, B. Wolf, P. Thalmeier, M. Gunther, W. Sixl, and G. Bruls, Phys. Lett. A **175**, 237 (1993).
[8]Y. Dubi and A. V. Balatsky, Phys. Rev. Lett. **106**, 086401 (2011).
[9]A. F. Santander-Syro, M. Klein, F. L. Boariu, A. Nuber, P. Lejay, and F. Reinert, Nat. Phys. **5**, 637 (2009).
[10]A. R. Schmidt, M. H. Hamidian, P. Wahl, F. Meier, A. V. Balatsky, J. D. Garrett, T. J. Williams, G. M. Luke, and J. C. Davis, Nature (London) **465**, 570 (2010).
[11]P. Aynajian, E. H. da Silva Neto, C. V. Parker, Y. Huang, A. Pasupathy, J. Mydosh, and A. Yazdani, Proc. Natl. Acad. Sci. **107**, 10383 (2010).
[12]J. G. Rodrigo, F. Guinea, S. Vieira, and F. G. Aliev, Phys. Rev. B **55**, 14318 (1997).
[13]A. V. Balatsky, A. Chantis, H. P. Dahal, D. Parker, and J. X. Zhu, Phys. Rev. B **79**, 214413 (2009).
[14]C. Pépin, M. R. Norman, S. Burdin, and A. Ferraz, Phys. Rev. Lett. **106**, 106601 (2011).
[15]H. Amitsuka, M. Sato, N. Metoki, M. Yokoyama, K. Kuwahara, T. Sakakibara, H. Morimoto, S. Kawarazaki, Y. Miyako, and J. A. Mydosh, Phys. Rev. Lett. **83**, 5114 (1999).
[16]N. P. Butch, J. R. Jeffries, S. Chi, J. B. Leão, J. W. Lynn, and M. B. Maple, Phys. Rev. B **82**, 060408 (2010).
[17]G. Motoyama, N. Yokoyama, A. Sumiyama, and Y. Oda, J. Phys. Soc. Jpn. **77**, 123710 (2008).
[18]R. Okazaki, M. Shimozawa, H. Shishido, M. Konczykowski, Y. Haga, T. D. Matsuda, E. Yamamoto, Y. Onuki, Y. Yanase, T. Shibauchi, and Y. Matsuda, J. Phys. Soc. Jpn. **79**, 084705 (2010).
[19]K. Haule and G. Kotliar, Nat. Phys. **5**, 796 (2009).
[20]K. H. Kim, N. Harrison, M. Jaime, G. S. Boebinger, and J. A. Mydosh, Phys. Rev. Lett. **91**, 256401 (2003).
[21]Y. Dalichaouch, M. B. Maple, J. W. Chen, T. Kohara, C. Rossel, M. S. Torikachvili, and A. L. Giorgi, Phys. Rev. B **41**, 1829 (1990).
[22]M. Yokoyama, H. Amitsuka, S. Itoh, I. Kawasaki, K. Tenya, and H. Yoshizawa, J. Phys. Soc. Jpn. **73**, 545 (2004).
[23]Y. Dalichaouch, M. B. Maple, M. S. Torikachvili, and A. L. Giorgi, Phys. Rev. B **39**, 2423 (1989).
[24]Y. Dalichaouch, M. B. Maple, R. P. Guertin, M. V. Kuric, M. S. Torikachvili, and A. L. Giorgi, Physica B **163**, 113 (1990).
[25]E. D. Bauer, V. S. Zapf, P. -C. Ho, N. P. Butch, E. J. Freeman, C. Sirvent, and M. B. Maple, Phys. Rev. Lett. **94**, 046401 (2005).
[26]N. P. Butch and M. B. Maple, Phys. Rev. Lett. **103**, 076404 (2009).
[27]H. M. Rietveld, J. Appl. Crystallogr. **2**, 65 (1969).
[28]A. Larson and R. V. Dreele, Los Alamos National Laboratory Report LAUR 86-748 (2000).
[29]B. H. Toby, J. Appl. Crystallogr. **34**, 210 (2001).
[30]A. Szytula, M. Slaski, B. Dunlap, Z. Sungaila, and A. Umezawa, J. Magn. Magn. Mater. **75**, 71 (1988).
[31]K. Kuwahara, H. Sagayama, K. Iwasa, M. Kohgi, S. Miyazaki, J. Nozaki, J. Nogami, M. Yokoyama, H. Amitsuka, H. Nakao, and Y. Murakami, Acta Phys. Pol. B **34**, 4307 (2003).
[32]K. Iki, G. Oomi, Y. Uwatoko, H. Takahashi, N. Mori, Y. Onuki, and T. Komatsubara, J. Alloys Compd. **181**, 71 (1992).
[33]R. Jaramillo, Y. Feng, J. Wang, and T. F. Rosenbaum, Proc. Natl. Acad. Sci. USA **107**, 13631 (2010).
[34]T. T. M. Palstra, A. A. Menovsky, and J. A. Mydosh, Phys. Rev. B **33**, 6527 (1986).
[35]E. Louis, A. De Visser, A. A. Menovsky, and J. J. M. Franse, Physica B + C **144**, 48 (1986).
[36]J. G. Park and B. R. Coles, J. Phys. Condens. Matter **6**, 1425 (1994).
[37]N. Hessel Andersen and H. Smith, Phys. Rev. B **19**, 384 (1979).
[38]M. B. Fontes, J. C. Trochez, B. Giordanengo, S. L. Budko, D. R. Sanchez, E. M. Baggio-Saitovitch, and M. A. Continentino, Phys. Rev. B **60**, 6781 (1999).